

## Self-association processes involving anthracene labeled phosphatidylcholines in model membrane

Frédéric Rodriguez <sup>a</sup>, Jean-François Tocanne <sup>b</sup>, André Lopez <sup>b,\*</sup>

<sup>a</sup> *Institut de Biologie Cellulaire et de Génétique du CNRS, 118 Route de Narbonne, 31062 Toulouse Cedex, France*

<sup>b</sup> *Laboratoire de Pharmacologie et Toxicologie Fondamentales du CNRS, Dept. III, 118 Route de Narbonne, 31062 Toulouse Cedex, France*

Received 28 October 1993; accepted in revised form 7 September 1994

### Abstract

When studying lipid–lipid or lipid–protein interaction in membranes, the correct interpretation of data obtained when using fluorescent phospholipid probes requires the best possible knowledge of probe behaviour in phospholipid membranes. Analysis of the translational dynamics and photochemical properties of the anthracene-labeled phosphatidylcholine (EAPC) shows that a self-association process occurs with this probe in the membrane at the ground state. This anthracene self-association is characterized and leads to a hypochromic effect which has been studied by means of ultraviolet absorption spectroscopy in unilamellar egg-yolk phosphatidylcholine (EggPC) vesicles. A model with indefinite linear self-association, in which each step has the same equilibrium constant, best describes the data. The equilibrium constant was found to be in the 300–500 M<sup>−1</sup> range and the complex lateral distribution pattern of EAPC in model membranes, which results from this self-association process, is characterized and seems to be mainly controlled by the amount of EAPC incorporated into the lipid bilayer.

**Keywords:** Anthracene; Phospholipid probe; Self-association; Membrane model; Spectroscopy (light absorption)

### 1. Introduction

Knowledge of a clear dynamic picture of lipid and protein organization in membranes remains a challenging problem in membrane biology. A direct ap-

proach to the study of lipid–lipid and lipid–protein interactions involves the labeling of membrane components with site-directed ligands carrying fluorescent and/or chemically reactive photosensitive groups [1]. For ten years we have suggested the use of 9-(2-anthryl)-nonanoic acid [2,3] or 8-(2-anthryl)-octanoic acid [4,5] and various corresponding anthryl/anthroyl-labeled phospholipids [2–5] for such studies.

The photochemistry and particularly the photodimerization of anthracene is one of the oldest known photochemical reactions [6,7]. This photo-re-

Abbreviations: EAPC: sn-1-acyl-sn-2,9-(2-anthryl)-nonanoylphosphatidylcholine; EggPC: egg yolk L- $\alpha$ -phosphatidylcholine; DPPC: dipalmitoyl phosphatidylcholine; FRAP: fluorescence recovery after photobleaching; OD: absorbance of the sample

\* Corresponding author.

action was chosen for its high specificity and the photochemical properties of the photodimers produced. After illumination at a wavelength of 360 nm, 9–9', 10–10' covalently bound dimers are formed, and these photo-products are not fluorescent. Under illumination at 260 nm, the dimers can be split into the native monomers.

Anthracene probes can be incorporated into membrane lipids by inserting anthracene-labeled lipids [8,9] or through metabolic incorporation of 9-(2-anthryl) nonanoic acid in both prokaryotic [10] and eukaryotic [11] cells. Anthracene-labeled lipids, which label the hydrophobic core of the membrane, are well suited for investigating membrane fluidity [12] and intramembraneous micro polarity [4,13], when measuring the lateral diffusion rate of lipids by FRAP experiments [9] or by following the kinetics of the photodimerization reaction [14], and for studying the lateral distribution of lipids in biological membranes by identification and counting of the photo-products which are formed between adjacent anthracene-labeled molecules [15].

However as for any probe approach, the purpose is to obtain structural information or characteristic parameters about the phospholipids which compose the host membrane, while the validity of fluorescence measurements is related to the fluorophore used and depends on the behavior of the lipid probes in the phospholipid surrounding. Thus all the knowledge about the disturbance of phospholipid molecular organization by the fluorescent lipid probe used is essential. The publication by Bredlow et al. which relates the changes brought about in the molecular packing of the host lipid by various fluorescent lipid tracers [16], illustrates reciprocal disturbance between the probe and the host phospholipid very clearly. Moreover, in this type of study, the probes are often presumed to be randomly distributed in the membrane without being affected by environmental factors of fluidity or polarity. However in the absence of lipid probes some phospholipid constituents of model membranes are not completely miscible [17], and in any case this question of miscibility becomes still more complex when lipid probes are introduced. Indeed when lateral distribution of a probe in a host membrane is investigated ideal miscibility is rarely observed. For example Blackwell et al. [18] have shown for pyrene-labeled lipids that the

excimer fluorescence in fluid membranes arises from an aggregated form of pyrene tracers and does not reflect controlled diffusion of monomer species in the formation of excimers. For a pyrene-labeled lipid Somerharju et al. [19] have again shown clearly that the partition of pyrene lipids between coexisting fluid and solid phases was always favourable to the fluid phase and that this preference took place independently of the head group of the host phospholipid. Various other attempts to analyze the lateral aggregation of lipophilic aromatic probes like pyren-phosphatidyl cholines [18,20,21] or diphenyl hexatrien-phosphatidylcholines [22–24] have also been studied.

Lateral aggregation of lipophilic probes is a critical problem which cannot be ignored when using fluorescent probes, so analysis of the behavior of a lipid probe is to be carried out whenever possible because the correct interpretation of data, obtained with these procedures, requires exact knowledge of the behaviour of the probe molecule firstly in relation to itself and secondly in relation to phospholipids in the host membrane. We report here on the study of lateral miscibility of anthracene-labeled phosphocholine (EAPC) in a model membrane of egg yolk phosphatidyl choline (EggPC).

## 2. Materials and methods

### 2.1. Chemicals

EggPC was purchased from Sigma (St. Louis, MO, USA), EAPC was synthesized from egg yolk lysolecithin, as previously described [2]. The purity of these compounds was checked by thin-layer chromatography on silica–gel plates (Merck, Darmstadt, Germany). Salts and solvents were of analytical grade.

### 2.2. Vesicle preparations

EAPC was added to EggPC at the desired molar ratio in chloroform solution. The lipid samples were dried by evaporation of chloroform, first under nitrogen and then for at least 2 hours under vacuum (1 Torr). The dried lipid mixtures were then dispersed in pure water at a final concentration of between 0.5

Table 1

Characteristic values of absorbance parameters when measurements are carried out with EAPC/EggPC membrane suspensions. Normalized absorbance (OD) (see materials and methods section) and molar absorption coefficients at wavelengths of 380 nm ( $OD_{380}$ ,  $\epsilon_{380}$ ) and 360 nm ( $OD_{360}$ ,  $\epsilon_{360}$ )

$\gamma_{EAPC}$ (%)	$[C_M](10^{-4})$	$OD_{380}(10^{-3})$	$\epsilon_{380}(M^{-1} cm^{-1})$	$\pm \Delta\epsilon(M^{-1} cm^{-1})$	$OD_{360}(10^{-3})$	$\epsilon_{360}(M^{-1} cm^{-1})$	$\pm \Delta\epsilon(M^{-1} cm^{-1})$
20	5	277.4	1386	13	326.9	1634	52
20	10	279.7	1398	13	323.6	1619	35
20	10	280.8	1405	13	330.7	1652	35
20	5	278.6	1383	< 13			
10	10	142.1	1421	26	160.3	1603	52
10	5	146.9	1469	26			
7.5	5	105.7	1408	38			
5	10	70.1	1402	32	80.7	1613	70
5	10	71.1	1423	51	81.5	1631	70
5	5	70.9	1417	32			
4	10	58.4	1460	32	69.1	1728	88
3	10	44.1	1469	38	48.8	1594	114
2.5	5	36.8	1474	64			
2	10	29.9	1495	51	36.7	1837	105
2	10	30.1	1508	64	34.8	1740	80
2	10	30.0	1501	51	35.8	1793	70
1	10	16.2	1624	64	17.4	1740	140
1	10	16.5	1649	90	18.2	1828	210
1	10	16.5	1649	64	18.2	1828	140
1	10	16.5	1649	90	18.6	1863	140
1	10	16.5	1649	64	19.5	1951	140
1	5	15.9	1598	64			
0.75	5	15.7	2097	90			
0.75	5	15.5	2066	90			
0.7	10	13.4	1915	75	13.3	1909	264
0.7	10	13.8	1970	77	13.7	1958	175
0.7	10	13.1	1878	77	15.3	2185	158
0.5	10	10.7	2139	83	13.0	2285	176
0.5	10	11.2	2242	83	11.6	2039	176
0.5	10	11.7	2345	83	12.0	2109	176
0.5	10	10.8	2165	83	12.4	2179	176
0.5	10	11.1	2217	90	12.6	2215	176
0.5	10	10.8	2165	103	14.0	2461	351
0.25	10	7.7	3093	128	7.0	2461	391
0.25	5	6.2	3196	128			
0.25	10	7.9	3196	141			
0.2	10	6.3	3158	154			
0.1	5	4.1	4124	322			
0.1	5	4.6	4640	322			
0.1	10	3.9	3995	257			

$10^{-3}$  M to  $1 \cdot 10^{-3}$  M, vortexed for 1 minute, sonicated for 3 minutes (under nitrogen) in pulsed mode (Branson sonifier) and then incubated at room temperature 4 to 8 hours. Using this procedure, relaxed small unilamellar vesicles (SUV) are produced, which best allow the preparation of liposomes with minimal turbidity, and in all cases comparable or lower (data not shown) to that obtained when lipid vesicles are prepared using the method of reverse-phase evaporation [25]. Using photon correlation spectroscopy apparatus (model N4MD, Coulter USA) the samples showed unimodal size distribution with a mean particle radius of 500 Å to 800 Å depending on the preparation.

### 2.3. Spectroscopic measurements

Absorbance measurements were performed with a Perkin-Elmer Lambda 5 spectrophotometer, at 20°C (thermostated cuvette holder). The absorbance difference between cuvette cell and air was measured and calibration at zero base line was carried out at the same wavelength. Absorbance of the sample (OD) was obtained by graphic deconvolution of absorption spectra recorded between 240 and 280 and 340 to 420 nm in order to eliminate absorption due to light scattering [26]. Each absorbance measurement was performed 3 to 5 times with a new phospholipid suspension with a phospholipid concentration in the range of  $0.5 \cdot 10^{-3}$  to  $1 \cdot 10^{-3}$  M. The values ( $\epsilon$ ) and uncertainties ( $\Delta\epsilon$ ) of molar absorption coefficients indicated in Table 1 are normalized at a total phospholipid concentration of  $1 \cdot 10^{-3}$  M. The extent of ( $\Delta\epsilon$ ) corresponds to the dispersion of ( $\epsilon$ ) calculated values obtained after analysis of each measurement of a new liposomal suspension.

### 2.4. Computer calculations

Calculations were performed using a non-linear least-squares package developed in this laboratory [27] and already used to analyze other types of data [28]. The merit function was expressed as a non-weighted sum of squares of residuals between a given model and experimental data. The parametric confidence intervals at 5% of error risk were calculated using a modified boundary method.

## 3. Basic considerations

### 3.1. Anthracene probe and general concepts

Three types of photo-reaction can be encountered in solutions with anthracene derivatives: dimerization, photo-oxidation and reaction with the environmental medium [6]. In apolar solutions or in anisotropic lipid phase mediums, photo-oxidation was negligible [2,3] and we never observed condensation of anthracene with unsaturated fatty acids of lecithin. Hence our attention focused on the main photochemical reaction, the dimerization of anthracene. Photodimerization involves the participation of one anthracene at singlet excited state and another at fundamental state [14,29]. When the anthracene ring is substituted by an *n*-acyl chain in the second position (EAPC has this structure), steric hindrance to coplanarity from ring hydrogens appears insignificant. Moreover when this happens and when the lipid probe is in an anisotropic membrane medium, the part of the alkyl substituent in the anthracene is on average closely aligned to the polarization of the first anthracene transition ( $^1A_1 \rightarrow ^1L_a$ ) [30]. Thus, it is in this case normal for the anthracene residue to cause minimum structural disturbance in surrounding lipids in the ground state or in the first excited state [2,12,13].

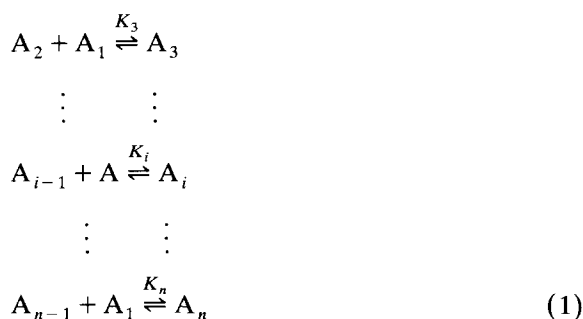
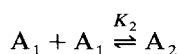
Moreover the anthracene group is well localized in the hydrophobe core of a lipid bilayer and does not display any looping back to the surface [12,13]. However some preliminary remarks are important, if we consider that the lipid probes are statistically distributed within the lipid matrix and diffuse laterally according to a free volume translation mechanism. (i) We will firstly consider the molecular packing of EAPC or EggPC. We can say that the lipid probe and the host lipid of a membrane have comparable molecular areas in a range of around  $60 \times 10^{-16}$  cm<sup>2</sup>/molecule at a lateral pressure of 25 mN/m and for a temperature of 20°C [2,26]. (ii) Secondly we will consider the translational diffusion coefficient of phospholipids in a leaflet of EggPC model membrane. It has a value of around  $3.5 \times 10^{-8}$  cm<sup>2</sup>/s [28]. By means of the two previous remarks we can calculate that the hopping frequency is  $1.7 \times 10^{-7}$  s<sup>-1</sup> or the time between two encounters is close to  $170 \cdot 10^{-9}$  s. (iii) Thirdly, the translational

dynamic parameters of EAPC or EggPC in the membrane lipids must now be compared with known photochemical properties of the anthracene group. Generally, the fluorescence life-time of 2-substituted anthracenes does not exceed  $5 \times 10^{-9}$  s [4,12,30]. Therefore for a probe to lipid molar incorporation ratio ( $\gamma_{\text{EAPC}}$ ) of 1% of EAPC in the membrane, with the above parameters one can calculate that around  $1.7 \times 10^{-5}$  collisions between two EAPC molecules will occur during the fluorescence life-time of anthracene. Even if the efficiency of the collision is maximum and leads to the formation of a photodimer each time, these kinetic parameters cannot explain the effectiveness of the observed dimerization process at this rate of high dilution of the anthracene probe. In other words, the anthracene groups of EAPC are necessarily pre-positioned in order to allow the photodimerization process to occur. The phospholipidic membranes (liposomes, multilayers, part of cell membranes) are anisotropic and ordered mediums with restricted degrees of molecular freedom as compared to a three dimensional solution. All these elements could cooperate to make the stacking process of anthracene rings of EAPC molecules easier.

If pre-associated dimers can exist before a photodimerization event, then we need to investigate: (i) the nature of the pre-association process, (ii) the number of EAPC molecules in a given temporary aggregate, (iii) the distribution of aggregates at a given EAPC incorporation ratio in a membrane, and finally, (iv) the consequences of these auto-association processes on the stationary fluorescence and photodimerization properties of anthracene-labeled lipids.

### 3.2. Self-association models

We wish to propose those self-association models which can be derived from studies of small hydrophobic molecules in aqueous solutions [31–33]. The self-association of anthryl labeled phospholipids noted A into aggregates of various sizes, in lipid bilayer, is described by the following set of equations:



In this reaction scheme,  $A_1$  represents the monomer,  $A_i$  stands for an aggregate consisting of  $i$  monomers,  $[A_1]$ ,  $[A_2]$ , ...  $[A_n]$ , stand for the corresponding concentration of each species and  $K_2$ ,  $K_3$ , ...  $K_n$  are the equilibrium constants of corresponding chemical equations. According to the law of the action of mass,

$$\begin{aligned} K_2 &= \frac{[A_2]}{[A_1] \cdot [A_1]} \\ K_3 &= \frac{[A_3]}{[A_2] \cdot [A_1]} \\ &\vdots \\ K_i &= \frac{[A_i]}{[A_{i-1}] \cdot [A_1]} \end{aligned} \quad (2)$$

This model contains too many parameters to be determined experimentally if extensive aggregation occurs. Moreover, anthracene is an oriented but uncharged large flat ring structure, and interactions between two different aromatic rings are directed by very short-range forces. It is physically reasonable to assert that there is no difference in the values of equilibrium constants for each step. We will therefore consider two models.

The first corresponding to indefinite self-association in which all equilibrium constants are equal ( $K_2 = K_3 = \dots K_i = K$ ). This is the definition for the classical associative isodesmic model [31]. Therefore,

$$K \cdot [A_1] = \frac{[A_i]}{[A_{i-1}]} = q \quad (3)$$

in which  $q$  is a dimensionless variable for this chemical equilibrium system.

The second, limiting the self-association process, is characterized solely by a di-association equation and is given later.

### 3.3. Self-association models and optical ultra-violet properties

EAPC has previously been spectroscopically characterized [2]. This molecule shows an ultra-violet spectrum similar to that of 2-substituted anthracene compounds with systems of bands  $p$  and  $\beta$ , and a hypochromic effect has already been reported when liposome membranes are composed by pure EAPC in gel state [3]. Conceptually, the absorption coefficient of EAPC lipids in phospholipid vesicles of EggPC, at a selected wavelength, depends on the specific absorption of each species of associated anthracene which label the lipid medium. Thus, we have to consider the different contributions of aggregates to the optical signal, at various wavelengths, when the EAPC/EggPC ratio is changing. Indeed, when an associated dimer is formed, the absorption coefficient for each monomer in the stack changes due to the interaction between the excited states in the presence of the electrostatic field. The resulting aggregate is 'asymmetric', and a rotary strength is induced due to the interaction between the transition dipoles of the two chromophores [34–36]. The next anthracene group, which aggregates with the previous dimer to form trimer, creates an additional change. A simple phenomenological description for the  $i$ -dependence of the molar absorption coefficient of the aggregates consists in the assumption that only a few interactions are responsible for the change in the optical parameters (Fig. 1). Only three types of contribution are expected to be necessary for the descriptions of the resulting molar absorption coefficient [31]:

- (i) The contribution of the free monomer molar absorption coefficient, noted  $\epsilon_{\text{mono}}$ .
- (ii) In a stack the contribution of the elementary unit at the end of an aggregate, noted  $\epsilon_{\text{ext}}$ .
- (iii) The contribution of all internal units of the stack, assumed to have the same molar absorption coefficient, noted  $\epsilon_{\text{int}}$ .

The expression of the individual molar concentrations of each  $n$ -mers is shown in Annex A1 for the general isodesmic model. Molar absorption coeffi-

cients, molar quantities and equilibrium constants are volumic in nature and are not directly measurable in a bilayer. A relatively simple procedure is given in Annex A2 showing how to calculate the effective molar concentration  $C_A$  of EAPC in membrane using the incorporation ratio  $\gamma_{\text{EAPC}}$  of EAPC. The values obtained for the total phospholipid concentration  $C_M = 0.99$  M and for  $C_A$ ,  $C_A = \gamma_{\text{EAPC}}/100$  are high but near those obtained in other studies [37]. They could reflect the relative over-concentration and restricted degrees of freedom in membrane media.

### 3.4. Isodesmic model

The calculated molar absorption coefficient  $\epsilon_{\text{calc}}$  for a given concentration  $C_A$  of anthracene-labeled phospholipid in a membrane is defined as:

$$\epsilon_{\text{calc}} = \alpha_{\text{mono}} \epsilon_{\text{mono}} + \alpha_{\text{ext}} \epsilon_{\text{ext}} + \alpha_{\text{int}} \epsilon_{\text{int}} \quad (4)$$

in which  $\alpha_{\text{mono}}$  is the molar fraction of the free monomer, noted  $\alpha_1$  in Annex A1.  $\alpha_{\text{ext}}$  and  $\alpha_{\text{int}}$  are respectively the molar fraction of anthracene units at the extremities and inside the aggregates. Because  $\alpha_{\text{mono}}$ ,  $\alpha_{\text{ext}}$ , and  $\alpha_{\text{int}}$  are the molar fraction of each species, their sum is equal to 1. It is possible in order to correlate each value of  $\alpha_{\text{mono}}$ ,  $\alpha_{\text{ext}}$ ,  $\alpha_{\text{int}}$  to  $C_A$ , to combine Eq. 4 and Eqs. 13–15 of Annex A1. Hence:

$$\alpha_{\text{mono}} = \frac{1}{KC_A} + \frac{1 - \sqrt{4KC_A + 1}}{2K^2C_A^2} \quad (5)$$

$$\alpha_{\text{ext}} = 2(1 - \alpha_{\text{mono}} - \alpha_{\text{mono}}KC_A)$$

$$\alpha_{\text{int}} = 1 - \alpha_{\text{mono}} - \alpha_{\text{ext}} = \alpha_{\text{mono}}(1 + 2KC_A) - 1$$

### 3.5. Di-association model

The formulation of equation in the case of a unique di-association process leads to a simpler expression of  $C_A$ :

$$C_A = [A_1] + 2[A_2] \quad (6)$$

thus in a molar fraction the same relation is written as:

$$1 = \alpha_{\text{mono}} + \alpha_{\text{dim}} \quad (7)$$

in which  $\alpha_{\text{mono}}$  can be expressed as a function of the total concentration by the relation:

$$\alpha_{\text{mono}} = \frac{C_{\text{mono}}}{C_A} = \frac{\sqrt{1 + 8KC_A} - 1}{4KC_A} \quad (8)$$

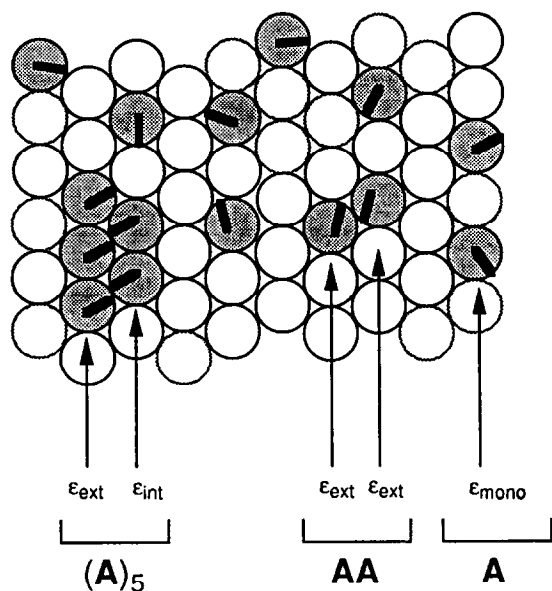


Fig. 1. Contributions of molar absorption coefficients in the case of an aggregate ((A)<sub>5</sub> = pentamer), a stacked pair (AA) and monomers (A) of EAPC molecules. Schematic upper view of a part of EggPC–EAPC membrane, the molecules are shown perpendicularly to the acyl chain axis. The grey positions are EAPC molecules the other loci are EggPC molecules. The bold oriented lines are anthryl planes of EAPC molecules showing how the stacking processes could occur in *n*-mers.

$$\alpha_{\text{dim}} = 1 - \alpha_{\text{mono}} = 1 - \frac{\sqrt{1 + 8KC_A} - 1}{4KC_A} \quad (9)$$

In this relation  $K$  is the equilibrium constant for the single association–dissociation step. Then the expression for the observed coefficient of absorption is:

$$\epsilon_{\text{calc}} = \epsilon_{\text{dim}} + \alpha_{\text{mono}} \cdot (\epsilon_{\text{mono}} - \epsilon_{\text{dim}}) \quad (10)$$

Knowing the concentration  $C_A$  of the labeled phospholipid, it is possible from the measurement of  $\epsilon_{\text{obs}}$  to calculate the different parameters  $K$ ,  $\epsilon_{\text{mono}}$ ,  $\epsilon_{\text{ext}}$ ,  $\epsilon_{\text{int}}$  in an iterative way using a non-linear least-squares program [27]. Then, the previous expression of  $\epsilon_{\text{calc}}$  (Eqs. 4 or 10), is taken as the model used to fit a set of measured values of  $\epsilon$  for different values of  $\gamma_{\text{EAPC}}$  in known solutions.

#### 4. Results and discussion

In Table 1, results of the absorption measurements at 380 nm and 360 nm are shown for various

EAPC incorporation ratios ( $\gamma_{\text{EAPC}}$ ) in Egg-PC small vesicles. The values of  $\gamma_{\text{EAPC}}$  are in the range of 0.2 to 20%. The corresponding molar absorption coefficient  $\epsilon_{380}$  and  $\epsilon_{360}$  showed ca. 2 to 3 fold increase with decreasing EAPC concentration. Measurements were difficult: (i) for low  $\gamma_{\text{EAPC}}$  values because in this case the optical density was low, (ii) and also for high  $\gamma_{\text{EAPC}}$  values because a light scattering band introduced a strong curve in the spectrum baseline. So, experimental uncertainties were not negligible for (j)  $\gamma_{\text{EAPC}}$  values lower than 1% and for (jj) the absorption band measured at 360 nm, and this was accounted for in results shown in Table 1. Therefore the uncertainty of each value of molar absorption coefficient indicated in Table 1 points out the calculated dispersion for each set of surfacic concentration  $\gamma_{\text{EAPC}}$  but measured at different total lipid concentrations. Moreover this hypochromic effect detected when  $\gamma_{\text{EAPC}}$  increase was not followed by a shift of a maximum wavelength of anthracene absorption bands. The effect seems to be due to a true auto-associative phenomenon in the case of EAPC in vesicles of EggPC.

The data in Table 1 was processed using the isodesmic model or the di-association model previously defined. The corresponding fitted curves are plotted in Fig. 2 and Fig. 3 and the solution values for each parameter are indicated in Table 2. The

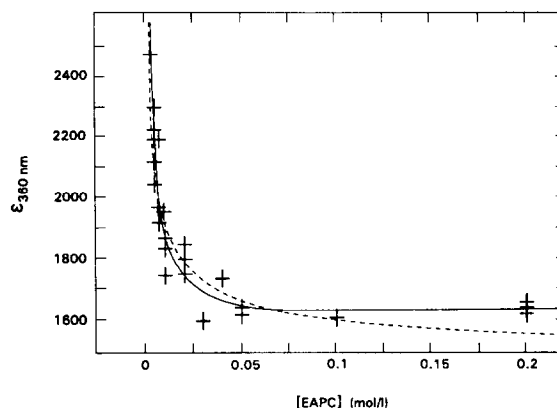


Fig. 2. Least squares fit of the molar absorption coefficient values of Table 1 measured at a wavelength of 360 nm using the isodesmic (continuous curve) and di-association (dashed curve) models. The ratio of EAPC incorporated in membrane of EggPC vesicles is expressed in molar concentration units of EAPC in small liposome membranes.

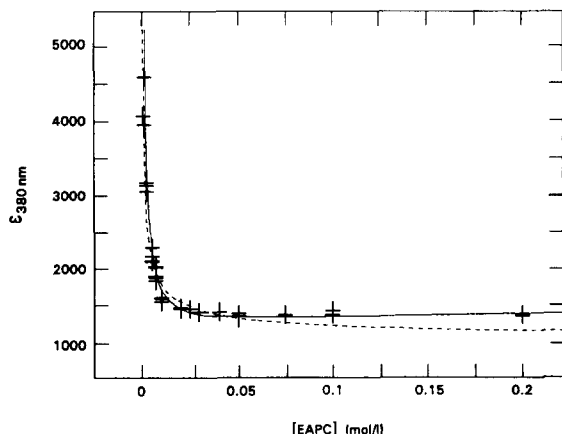


Fig. 3. Least-squares fit of the molar absorption coefficient values of Table 1 measured at a wavelength of 380 nm using the isodesmic (continuous curve) and di-association (dashed curve) models. The ratio of EAPC incorporated in membrane of EggPC vesicles is expressed in molar concentration units of EAPC in small liposome membranes.

plots show in each case that the isodesmic model describes the data better. Moreover, the di-association model gives physically unreasonable values for

optical and thermodynamic parameters. So, the di-association model fails to be an explicative model for the self association of anthryl-lipid fluorophore in model membranes. If the quality of the least-squares fit is better for the indefinite model, are there physical reasons for favouring this model? In the case of pyrene probes, di-association models have been used regarding the fluorescence properties of pyrene and excimer formation [30]. In the case of diphenyl hexatriene phospholipid probes deterministic models are used with a limited number of association steps limited to two [22,23]. Our results show that with EAPC self-association of the probe is not in fact limited to the dimer stage. We note also that the data at 360 nm is more dispersed than at 380 nm, probably due to the difficulties in the measurement of the central band of anthracene *p*-system, but this did not disturb fundamentally the model (Table 2) [26].

#### 4.1. Calculated parameters

The calculated parameters and results of calculation are summed up in Table 2. We shall mainly discuss the results for the isodesmic model. The

Table 2

Optical and thermodynamic parameters for EAPC self-association computed using the infinite self-association (isodesmic) or di-association (dimer) models. The parameter confidence intervals (PCI) are calculated for a 5% error risk (5%), the values of  $K$  and  $\epsilon$  are expressed in  $M^{-1}$  and in  $M^{-1} cm^{-1}$  units, respectively

Wavelength	Parameters			
	Name	Value	PCI (5%)	
			Min	Max
<i>Isodesmic model</i>				
380 nm	$K$	465	415	516
	$\epsilon_{\text{mono}}$	7531	7292	7774
	$\epsilon_{\text{int}}$	1655	1476	1834
	$\epsilon_{\text{ext}}$	100	13.5	238
360 nm	$K$	271	242	301
	$\epsilon_{\text{mono}}$	3864	3740	4280
	$\epsilon_{\text{int}}$	1719	1665	1905
	$\epsilon_{\text{ext}}$	1164	1038	1290
<i>Dimer model</i>				
380 nm	$K$	985672	492836	1092125
	$\epsilon_{\text{mono}}$	105773	102387	132850
	$\epsilon_{\text{ext}}$	1030	913	1292
360 nm	$K$	1464127	1089311	1622254
	$\epsilon_{\text{mono}}$	62139	55422	68843
	$\epsilon_{\text{ext}}$	1448	1401	1494



values of the molar absorption coefficient of the monomer agree with measured values in protic or aprotic solvents. In the case of ethanol, the values are:  $\epsilon_{378} = 4800 \text{ M}^{-1} \text{ cm}^{-1}$  and  $\epsilon_{358} = 5842 \text{ M}^{-1} \text{ cm}^{-1}$  [2]. In hexane and for methyl 9-(2-anthryl) nonanoyl, we have measured  $\epsilon_{376} = 4970 \text{ M}^{-1} \text{ cm}^{-1}$  and  $\epsilon_{357} = 5666 \text{ M}^{-1} \text{ cm}^{-1}$  for identical solution  $C_A$  values. The  $\epsilon$  values for the nonsubstituted anthracene group in ethanol are near  $8000\text{--}8500 \text{ M}^{-1} \text{ cm}^{-1}$  and reach  $9000 \text{ M}^{-1} \text{ cm}^{-1}$  for  $-9$ ,  $-10$  substituted anthracenes (when the substitution is in the polarization axis corresponding to the  $A \rightarrow {}^1L_a$  electronic transition) [30,38,39]. For EAPC in liposomes we have calculated a value of around

$3900 \text{ M}^{-1} \text{ cm}^{-1}$  at 360 nm and  $7500 \text{ M}^{-1} \text{ cm}^{-1}$  at 380 nm (Table 2). On the other hand, the value of the molar absorption coefficient found at 360 nm is certainly quite low, presumably due to the difficulty in the analysis of spectra in presence of a non-negligible light scattering band.

Relatively high association constant values are found in the isodesmic model ( $K$  ca.  $500 \text{ M}^{-1}$ ), by comparison, much lower values of around 50 were found for purine and pyrimidine compounds in aqueous solutions [31]. However, values of  $1500 \text{ M}^{-1}$  have been reported in the case of daunomycin [33] which is a poly-aromatic anthracyclin which displays some analogies with anthracene. In the case of mem-

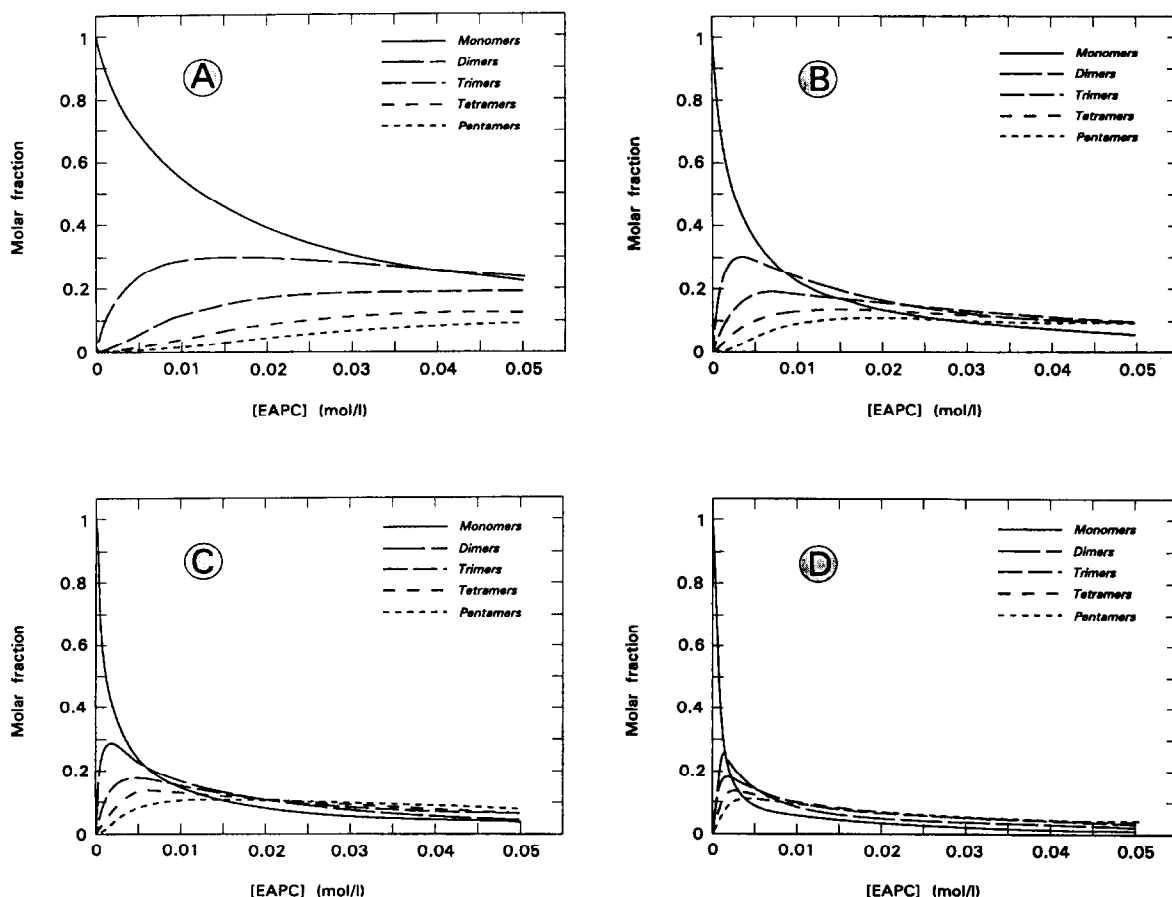


Fig. 4. Calculation of  $n$ -mer distribution up to pentamers versus molar concentration of EAPC in membranes and for four values of the association constant  $K$ :  $K = 50 \text{ M}^{-1}$  (A),  $K = 250 \text{ M}^{-1}$  (B),  $K = 500 \text{ M}^{-1}$  (C),  $K = 1500 \text{ M}^{-1}$  (D). The distribution in each curve, is given using molar fractions (monomers, dimers, trimers, tetramers, pentamers) and calculated using Eq. (14) for monomers and Eq. (15) for  $n$ -mers.

branes, with phosphatidylcholines carrying diphenylhexatrien groups, values of association constants of  $270 \text{ M}^{-1}$  have been reported [23]. So, the anthracene substituant in EAPC displays comparable behaviour to diphenylhexatriene in membrane.

#### 4.2. Behaviour of EAPC in membranes

Fig. 4 shows calculated  $n$ -mers distribution for  $K$  values of  $50 \text{ M}^{-1}$  (A),  $250 \text{ M}^{-1}$  (B),  $500 \text{ M}^{-1}$  (C) and  $1500 \text{ M}^{-1}$  (D) using the molar fraction calculations defined in the theoretical section. The gap between the calculated  $K$  values of  $465 \text{ M}^{-1}$  and  $271 \text{ M}^{-1}$ , respectively, at 380 nm and 360 nm could be explained by the difference in the experimental ease of recording data at these two wavelengths. However in the end, the differences in  $K$  have little consequence on the molecular distribution of the  $n$ -mers as shown in the Fig. 4B and Fig. 4C, which indicated for a variation of  $K$  value from  $250 \text{ M}^{-1}$  to  $500 \text{ M}^{-1}$  the distribution pattern is not very different, and though  $K$  values are different, the EAPC distributions are in a state in which the monomers are not predominant. In fact, EAPC molecules mainly take part in molecular aggregates of more than two units. We show that the distribution of EAPC  $n$ -mers at current incorporation ratios (1–3%) in model systems is quite complex. A trend towards a limit value of EAPC is to be expected in the number of EAPC in an aggregate but this model does not allow us to estimate it. Another result is the particular evolution of molar fractions for values of  $\gamma_{\text{EAPC}}$  between 0.5 and 1%, and chaotic behaviour of EAPC in photodimerization studies has been recorded near this incorporation ratio (data not shown). These are the first elements showing that self-association of EAPC could intervene in photodimerization process.

#### 4.3. Perspectives and conclusion

This data shows the particular behaviour of EAPC in phospholipidic membranes. At all incorporation ratios it seems that aggregates exist, in the form of dimers for  $\gamma_{\text{EAPC}}$  values  $< 0.5\%$ , and in the form of  $n$ -mers for the highest concentrations. In all cases, this self-association is dynamic.

Can these aggregation processes be expected for other phospholipid probes carrying aromatic fluorophores in phospholipid membranes? Pyrene-labeled molecules form visible dimers in the excited state (excimers) [40], which can be explained following a bimolecular reaction and if it is diffusion-controlled, the reaction rate constant can be related to the diffusion coefficient of pyrene. In a membrane this assumption has been extrapolated from the studies in organic solvents and has not been adequately tested by mean of studies of the concentration dependence of the fluorescence-decay kinetics, and significantly, Blackwell et al. [18] have shown that excimer fluorescence in membranes arises from an aggregated form of pyrene and does not reflect diffusion controlled excimer formation. Moreover pre-existing aggregates in the ground-state as precursors to fluorescence emission at excimer fluorescence wavelength have also been suggested by Bohorquez and Patterson as explaining the initial behaviour of excimer fluorescence decay ([41] and references cited herein). Yes, these aggregation processes in the ground-state can be expected for phospholipid probes carrying aromatic fluorophores in hydrophobe part of membranes.

From a dynamic point of view, the self-association of EAPC does not mean that the probe is segregated in a micro-phase in the membrane. Values of second-order association rate constants of  $5 \times 10^{-8} \text{ M}^{-1} \text{ s}^{-1}$  and  $5 \times 10^{-7} \text{ s}^{-1}$  for the dissociation counterpart have been reported [42]. In the case of collisional rate constants for pyrene in membranes, values of  $1 \times 10^{-6} \text{ M}^{-1} \text{ s}^{-1}$  have mainly been reported [18]. We can therefore hold the view of a bilayer in which partial formation–destruction of aggregates occurs very rapidly. Distribution and size of the aggregates are mainly directed by the incorporation ratio of EAPC in the bilayer.

If we agree with the assumption of collisional events with a characteristic time constant of around  $10^{-6}$ – $10^{-7} \text{ s}$ , the dynamic association processes could not ‘interfere’ with the photochemical properties of the probes because the life-time of the probe in EAPC is lower than  $10^{-8} \text{ s}$  and the measured fluorescence signal is representative of probe distribution which is in this case directed by the equilibrium constant of molecular self-association. So, dynamic parameters such as the diffusion coefficient

are not dependent on the spatial distribution of the probe if we accept that the distribution of  $n$ -mers is random.

The problem is the same if we now consider the study of the lateral distribution of phospholipids in a biological membrane after metabolic incorporation of the anthracene fatty acid and photodimerization [15]. When a photodimer has been formed, stacked  $n$ -mers may dissociate and form a new aggregate of probes. Probe redistribution occurs and thus the self-association process does not disturb the final distribution of dimers.

If we now consider micro-structural information obtained by a study of the kinetic dimerization constant, its variation according to the composition of the membrane and its state may be a more complex phenomenon. Work is being carried out in the laboratory to clarify this. The goal now is not only to characterize the auto-association processes in the case of other anthracene-lipid probes but also to clarify the influences of these processes in quantitative fluorescence studies using these fluorescent probes. Accordingly, our view of probe behaviour could be quite different from what we know to date.

## 5. Annex A1

### 5.1. Expression of the individual molar concentration and molar ratios of EAPC $n$ -mers

$C_A$  is the total molar concentration of anthracene labeled phospholipid in a membrane lipid phase, and  $[A_i]$  the molar concentration of the aggregate consisting of  $i$  EAPC molecules. In the case of indefinite self-association mass conservation can be written as:

$$C_A = \sum_{i=1}^{i=n} i \cdot [A_i] \quad (11)$$

Using molar ratio, noted  $\alpha$ , instead of concentration for each aggregate, the mass conservation equation becomes:

$$1 = \alpha_1 + \alpha_2 + \cdots \alpha_i + \cdots \alpha_n \quad (12)$$

in which,

$$\alpha_i = i \cdot \frac{[A_i]}{C_A} \quad (13)$$

For the isodesmic model, it is possible to obtain a relationship between  $[A_1]$  and  $C_A$  after selection of realistic physical conditions for the variable  $q$  ( $0 < q < 1$ ). Therefore the expression of the monomer concentration is calculated by reference to the total concentration in the equation:

$$[A_1] = \frac{1}{K} + \frac{1 - \sqrt{4KC_A + 1}}{2K^2 C_A} \quad (14)$$

The other  $n$ -mer concentrations  $[A_i]$  are calculated applying the law of the action of mass:

$$[A_i] = i \cdot (K)^{i-1} \cdot [A_1]^i \quad (15)$$

## 6. Annex A2

### 6.1. Expression of effective molar concentrations of EAPC in phospholipid bilayer

The calculations for molecular species in the membrane, are carried out using volumic concentration units (i.e. expressions of  $[A_i]$ ,  $C_A$  of  $K$ ), but membrane are a quasi 'bi-dimensional' media. The idea of giving the membrane a third dimension by introducing membrane thickness has already been used for fluorescent probes embedded in the lipid matrix [18,37,43]. The key to the problem is to know as closely as possible the value of the total concentration of phospholipid  $C_M$  (hosts and probes) in the membranes of the sample, expressed in  $\text{mol l}^{-1}$ .

The average molecular weight of EggPC is  $M_w = 785 \text{ g/mole}$  [43], and corresponds to 80% at acyl chain of  $C_{16}$  with one, two or three in saturations. On the surface of pure water at  $\Pi$  between 20–25 mN/m the average of the total interface film thickness (of this phospholipid medium in expanded phase state) is nearly the same value ( $M_t$ ) as this parameter for the DPPC in condensed phase state:  $25.3 \times 10^{-8} \text{ cm}$  [44]. Moreover we have estimated the molecular area  $M_a$  at this lateral pressure, from the measurement of a compression isotherm, it is  $60 \times 10^{-16} \text{ cm}^2$  [26]. The volume  $V_p$  of one mole of phospholipid is then known,  $V_p = M_t \cdot M_a \cdot N$  in which  $N$  is Avogadro's number. So, we can calculate the volumic weight of a mole of lipid in all phospholipid bilayers of the sample:  $\rho = M_w/V_p = 0.78 \times 10^3 \text{ g l}^{-1}$  or

the molar concentration  $C_M = 0.995$  M of phospholipid per membrane unit volume. Therefore, the value of the molar concentration of probe EAPC in the EggPC bilayer can be calculated knowing  $\gamma_{EAPC}$  the incorporation ratio of EAPC:

$$C_A = \frac{\gamma_{EAPC}}{100} \cdot C_M = \frac{\gamma_{EAPC}}{100} \quad (16)$$

in which the incorporation ratio of EAPC in a membrane is expressed in percentage units. The value of  $C_M$  is reckoned to an approximate value of 1 which is not unreasonable in regard to experimental approximations of values.

### Acknowledgements

We thank John Robb for checking the English of the manuscript.

### References

- [1] K. Jacobson, E. Elson, D. Koppel and W. Webb, *Fed. Proceed.*, 42 (1983) 72.
- [2] J. de Bony and J.F. Tocanne, *Chem. Phys. Lipids*, 32 (1983) 105.
- [3] J. de Bony and J.F. Tocanne, *Eur. J. Biochem.*, 143 (1984) 373.
- [4] E. Pérochon, A. Lopez and J.F. Tocanne, *Chem. Phys. Lipids*, 59 (1991) 17.
- [5] E. Pérochon and J.F. Tocanne, *Chem. Phys. Lipids*, 58 (1991) 7.
- [6] E.J. Bowen and D.W. Tanner, *Trans. Faraday Soc.*, 51 (1955) 475.
- [7] I. Fritzsche, *J. Prakt. Chem.*, 101 (1987) 333.
- [8] J.C. Kader, M. Julienne and C. Vergnolle, *Eur. J. Biochem.*, 139 (1984) 411.
- [9] L. Dupou, A. Lopez and J.F. Tocanne, *Eur. J. Biochem.*, 171 (1988) 669.
- [10] M. Welby and J.F. Tocanne, *Biochim. Biophys. Acta*, 689 (1982) 173.
- [11] L. Dupou, J. Teissié and J.F. Tocanne, *Eur. J. Biochem.*, 154 (1986) 171.
- [12] M. Vincent, J. Gallay, J. de Bony and J.F. Tocanne, *Eur. J. Biochem.*, 150 (1985) 341.
- [13] E. Pérochon, A. Lopez and J.F. Tocanne, *Biochemistry*, 31 (1992) 7672.
- [14] X. Ferrières, A. Lopez, A. Altibelli, L. Dupou, J.L. Lagouanelle and J.F. Tocanne, *Biophys. J.*, 55 (1989) 1081.
- [15] J. de Bony, A. Lopez, M. Gilleron, M. Welby, B. Rousseau, J.P. Beaucourt and J.F. Tocanne, *Biochemistry*, 28 (1989) 3728.
- [16] A. Bredlow, H.J. Galla and L.D. Bergelson, *Chem. Phys. Lipids*, 62 (1992) 293.
- [17] S. Mabrey and J.M. Sturtevant, *Proc. Natl. Acad. Sci.*, 73 (1976) 3862.
- [18] M.F. Blackwell, K. Gounaris and J. Barber, *Biochim. Biophys. Acta*, 858 (1986) 221.
- [19] P. Somerharju, J. Virtanen, K. Eklund, P. Vainio and P. Kinnunen, *Biochemistry*, 24 (1985) 2773.
- [20] M. Sassaroli, M. Vauhkonen, D. Perry and J. Eisinger, *Biophys. J.*, 57 (1990) 281.
- [21] M. Vauhkonen, M. Sassaroli, P. Somerharju and J. Eisinger, *Biophys. J.*, 57 (1990) 291.
- [22] D.A. Barrow and B.R. Lentz, *Biophys. J.*, 48 (1985) 221.
- [23] B.R. Lentz and S.W. Burgess, *Biophys. J.*, 56 (1989) 723.
- [24] E. Kalb, F. Paltauf and A. Hermetter, *Biophys. J.*, 56 (1989) 1245.
- [25] F. Szoka, F. Olson, T. Heath, W. Vail, E. Mayhew and D. Papahadjopoulos, *Biochim. Biophys. Acta*, 601 (1980) 559.
- [26] F. Rodriguez, *Approche de l'organisation et de la dynamique des lipides membranaires par photodimerisation de sondes phospholipidiques marquées à l'anthracène*, Thèse doctorat d'Université, Toulouse, France (1992).
- [27] F. Rodriguez, A. Altibelli and A. Lopez, *CABIOS*, 10 (1994) 145.
- [28] A. Lopez, L. Dupou, A. Altibelli, J. Trotard and J.F. Tocanne, *Biophys. J.*, 53 (1988) 963.
- [29] J. de Bony, G. Martin, M. Welby and J.F. Tocanne, *FEBS (Fed. Eur. Biochem. Soc.) Lett.*, 174 (1984) 1.
- [30] J.B. Birks, in J.B. Birks (Editor), *Photophysics of Aromatic Molecules*, Wiley Interscience, London (1970), pp. 1–82.
- [31] M.P. Heyn and R. Bretz, *Biophys. Chem.*, 3 (1975) 35.
- [32] E. Martinez, M. Rico and J. Santoro, *Ann. Quim.*, 79 (1983) 22.
- [33] J.B. Chaires, N. Dattagupta and D.M. Crothers, *Biochemistry*, 21 (1982) 3927.
- [34] J.A. Schellman, *Accounts Chem. Res.*, 1 (1968) 144.
- [35] I. Tinoco, *J. Rad. Res.*, 20 (1963) 133.
- [36] C.A. Bush, in P.O.P. Ts'o (Editor), *Basic Principles in Nucleic Acid Chemistry*, Academic Press, New York, Chapter 2, 1974, p. 91.
- [37] E. London and G.W. Feigenson, *Biochemistry*, 20 (1981) 1932.
- [38] R.A. Friedel and M. Orchin, in *Ultraviolet Spectra of Organic Compounds*, Wiley, New York, 1951, pp. 50–54.
- [39] T.C. Werner, T. Matthews and B. Soller, *J. Phys. Chem.*, 80 (1976) 533.
- [40] J.B. Birks, in G. Porter (Editor), *Progress in Reaction Kinetics*, Pergamon Press, Oxford, 1970, p. 181.
- [41] M. Bohorquez and L.K. Patterson, *J. Phys. Chem.*, 92 (1988) 1835.
- [42] D. Pörschke and F. Eggers, *Eur. J. Biochem.*, 26 (1972) 490.
- [43] M.D. Yeager and G.W. Feigenson, *Biochemistry*, 29 (1990) 4380.
- [44] N.H. Tattrie, J.R. Bennet and R. Cyr, *Can. J. Biochem.*, 46 (1986) 819.